Available online at www.sciencedirect.com
SCIENCE DIRECT®
Journal of Sound and Vibration 288 (2005) 81–90
JOURNAL OF SOUND AND VIBRATION
www.elsevier.com/locate/jsvi

Equilibria and vibration of a heavy pinched loop

S. Santillan[a], L.N. Virgin[a,*], R.H. Plaut[b]

[a]*Department of Mechanical Engineering and Materials Science, Duke University, Box 90300, Duke Durham, NC 27708-0300, USA*
[b]*Charles E. Via, Jr. Department of Civil and Environmental Engineering, Virginia Polytechnic Institute and State University, Blacksburg, VA 24061-0105, USA*

Received 15 July 2004; received in revised form 16 November 2004; accepted 18 December 2004
Available online 25 February 2005

Abstract

A thin strip is bent such that the two ends are brought together and clamped (pinched) to form a teardrop shape. The clamped end is held at various angles with the loop either upright, horizontal, downward, or halfway between these positions. The length of the loop is increased, and the resulting equilibrium shapes, as well as small in-plane vibrations about equilibrium, are investigated analytically and experimentally. When the loop is held upright, in-plane buckling occurs at a critical length, and subsequent postbuckling deflections can be large. For the other orientations, except the hanging one, deflections also become large as the length is increased. In the analysis, the strip is assumed to be an inextensible elastica which is unstrained when straight, and its self-weight is included. A shooting method is applied to obtain numerical solutions to the nonlinear equilibrium boundary value problem and the linear vibration boundary value problem. Polycarbonate strips are used in the experiments, and data are acquired with a laser vibrometer. The experimental deflections, frequencies, and mode shapes exhibit excellent agreement with the analytical solutions.

*Corresponding author. Tel.: +1 919 660 5342; fax: +1 919 660 8963.
E-mail address: l.virgin@duke.edu (L.N. Virgin).

0022-460X/$ - see front matter © 2005 Elsevier Ltd. All rights reserved.
doi:10.1016/j.jsv.2004.12.016

1. Introduction

The ends of a straight, thin, uniform, flexible strip are bent until they meet, and are clamped together. The strip then forms a teardrop shape, as shown in Fig. 1, and will be called a pinched loop. One application of such a pinched loop is in the loop tack test for adhesive tapes [1,2]. The adhesive is on the outside surface of the loop or on a flat surface. The loop is brought into contact with the surface and then pulled away. The same shape as the pinched loop also occurs in some buckling problems, such as: (1) when the ends of a clamped–clamped beam are moved toward each other until self-contact occurs between the two sides of the buckled shape [3,4]; (2) when a similar but asymmetric configuration occurs if a heavy fabric on a table is compressed and wrinkled [5]; and (3) when a bent strip is pushed onto a flat rigid surface [6]. A thin strip with pinned boundary conditions under axial compression was investigated in Ref. [7].

Equilibrium shapes and in-plane vibrations of a pinched loop are investigated analytically and experimentally here. The clamped end is oriented at five different angles from the horizontal: $\pi/2, \pi/4, 0, -\pi/4$, and $-\pi/2$ rad, where $\pi/2$ means that the loop is upright, 0 means that it is horizontal, and $-\pi/2$ means that the loop hangs vertically from its clamped support. The weight of the loop is included in the analysis, and the length of the loop is varied. Equilibrium configurations and the first four vibration frequencies and modes are determined.

If the loop is in the upright configuration and its length is increased, the deflections remain symmetric until in-plane buckling occurs at a critical length, and postbuckling shapes and frequencies are computed and measured, as well as those under prebuckling conditions. For the other orientations, deflections increase as the length is increased, with no buckling occurring. For the downward configuration, deflections remain symmetric as the length is varied.

In the analysis, formulated in Section 2, the loop is modeled as an inextensible elastica. Numerical results are obtained with the use of a shooting method. In the experiments, described in Section 3, the strips are made of polycarbonate and have various thicknesses and lengths. The analytical and experimental results, presented in Section 4, show excellent correlation. Concluding remarks are given in Section 5.

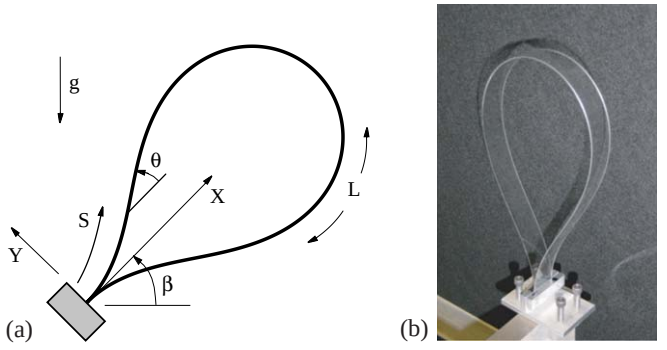

Fig. 1. (a) Geometry of pinched loop; (b) photographic image of experimental set-up.

2. Analytical formulation

The strip is assumed to be an elastica, which is thin, flexible, inextensible, unshearable, and unstrained when straight. It has length L, constant bending stiffness EI, and constant weight W per unit length. As shown in Fig. 1(a), points on the loop have coordinates $X(S,T)$ and $Y(S,T)$ where S is the arc length and T is time. The X-axis is parallel to the loop at the clamped end and has angle β with the horizontal, and the angle of rotation of the strip from the X-axis at arc length S is $\theta(S,T)$.

The internal forces in the loop, parallel to the $-X$ and $-Y$ axes on a positive face in the upper portion, respectively, are $P(S,T)$ and $Q(S,T)$, and the bending moment, which is proportional to the curvature, is $M(S,T)$. To put the analysis in nondimensional terms without involving the length L, define

$$a=(EI/W)^{1/3},\quad l=L/a,\quad x=X/a,\quad y=Y/a,\quad s=S/a,$$
$$p=Pa^2/EI,\quad q=Qa^2/EI,\quad m=Ma/EI,\quad t=T\sqrt{g/a},\quad \omega=\Omega\sqrt{a/g}, \tag{1}$$

where Ω is a dimensional vibration frequency.

Based on geometry, the moment–curvature relation $M=EI\partial\theta/\partial S$, and dynamic equilibrium, the governing nondimensional equations are

$$\partial x/\partial s=\cos\theta,\quad \partial y/\partial s=\sin\theta,$$
$$\partial\theta/\partial s=m,\quad \partial m/\partial s=q\cos\theta-p\sin\theta,$$
$$\partial p/\partial s=-\sin\beta-\partial^2x/\partial t^2,\quad \partial q/\partial s=-\cos\beta-\partial^2y/\partial t^2. \tag{2}$$

The weight per unit length of the loop does not appear explicitly in these equations and damping is neglected in the analysis.

The variables are written in the form

$$x(s,t)=x_e(s)+x_d(s)\sin\omega t,\quad y(s,t)=y_e(s)+y_d(s)\sin\omega t,$$
$$\theta(s,t)=\theta_e(s)+\theta_d(s)\sin\omega t,\quad m(s,t)=m_e(s)+m_d(s)\sin\omega t,$$
$$p(s,t)=p_e(s)+p_d(s)\sin\omega t,\quad q(s,t)=q_e(s)+q_d(s)\sin\omega t, \tag{3}$$

where the subscripts "e" and "d" denote equilibrium and dynamic, respectively, and the dynamic quantities will be assumed to be small.

For equilibrium, the governing equations are

$$x_e'=\cos\theta_e,\quad y_e'=\sin\theta_e,$$
$$\theta_e'=m_e,\quad m_e'=q_e\cos\theta_e-p_e\sin\theta_e,$$
$$p_e'=-\sin\beta,\quad q_e'=-\cos\beta. \tag{4}$$

Eqs. (4) lead to the relations

$$p_e(s)=p_0-s\sin\beta,\quad q_e(s)=q_0-s\cos\beta, \tag{5}$$

where p_0 and q_0 are constants.

After making use of Eqs. (5), Eqs. (4) are solved numerically using a shooting method [8] with the subroutines *NDSolve* and *FindRoot* in *Mathematica* [9]. The length l and angle β are specified,

and the known boundary conditions at $s = 0$ are $x_e(0) = y_e(0) = \theta_e(0) = 0$. The quantities $m_e(0), p_0$, and q_0 are varied until $x_e(l) = y_e(l) = 0$ and $\theta_e(l) = -\pi$ with sufficient accuracy. For the cases $\beta = \pi/2$ and $-\pi/2$, p_0 is not an unknown but is equal to $0.5l$ and $-0.5l$, respectively.

If the weight were neglected, then for any orientation, p_e would be zero and the bending moment $m_e(0)$ at the clamped end, the nondimensional length l, and the (constant) internal force q_e would be related by $m_e(0) = 6.05526/l = -0.96163(q_e)^{1/2}$ [10].

For small in-plane vibrations about equilibrium, Eqs. (3) are substituted into Eqs. (2) and nonlinear terms in the dynamic variables are neglected. After utilizing Eqs. (4), this leads to the linear vibration equations

$$\begin{aligned} &x_d' = -\theta_d \sin\theta_e, \quad y_d' = \theta_d \cos\theta_e, \\ &\theta_d' = m_d, \quad m_d' = (q_d - p_e\theta_d)\cos\theta_e - (p_d + q_e\theta_d)\sin\theta_e, \\ &p_d' = \omega^2 x_d, \quad q_d' = \omega^2 y_d. \end{aligned} \tag{6}$$

A shooting method is used again, with $x_d(0) = y_d(0) = \theta_d(0) = 0$. Since the modal amplitude is arbitrary, $m_d(0)$ is specified, for example, and $p_d(0), q_d(0)$, and ω are varied until $x_d(l) = y_d(l) = \theta_d(l) = 0$. Initial guesses for the nondimensional frequency ω are chosen in different ranges to compute the first four frequencies and the corresponding modes.

3. Experiments

Polycarbonate strips with various thicknesses and lengths were utilized in the experiments. The modulus of elasticity E was 2.4 GPa, the specific weight was 11.2 $\mathrm{kN/m^3}$, the width was 25.4 mm, and four thicknesses were used, ranging from 0.508 to 1.524 mm. The strips were bent into the appropriate configuration and clamped between two aluminum plates, which were mounted perpendicularly on a single plate. The orientation of the clamped end was adjustable. An example of an upright loop is shown in Fig. 1(b).

In the equilibrium configuration, the horizontal and vertical deflections of the midpoint of the loop were tracked as the length was increased. For the upright loop ($\beta = \pi/2$), until the critical length was reached, vertical deflections were small and the horizontal midpoint deflection was negligible. Large postbuckling deflections were observed as the length was increased beyond its critical value. There is no critical length (i.e., bifurcation) for other orientations. For the orientations $\beta = \pi/4, \beta = 0$ (i.e., horizontal), and $\beta = -\pi/4$, the length was increased a significant amount and large deflections occurred. For the hanging loop ($\beta = -\pi/2$), vertical deflections were small and the horizontal midpoint deflection was negligible.

The behavior of small-amplitude vibrations about the equilibrium configuration was then examined. A point-to-point laser vibrometer (*Ometron VH*300+) measured the vibration in terms of velocity near the support. Preliminary frequency spectra indicated that the motion was strongly influenced by the first four frequencies and also confirmed that damping was light, which justified the exclusion of damping in the analytical formulation. Over the appropriate frequency range, multiple data sets were taken and averaged for each strip length and orientation. For each set of measurements, the strip was excited manually in varying directions and locations along the strip.

Frequencies were tracked as a function of the length of the loop. For the upright loop, data were acquired under both prebuckling and postbuckling conditions.

For modal analysis, it was necessary to record both the loop response to excitation and the time series corresponding to the excitation. Employing a modal impact hammer (*Endevco* 2302-50) and *ME'scope VES* (*Vibrant Technology*, *Inc.*), the input and output time series were used to obtain a frequency response function for each measurement. For the specific mode shape study, the thickness chosen was 0.508 mm and the strip was clamped in the upright position. Measurements were taken at 30 points along the strip. The laser vibrometer was adjusted to measure at each of these points in the same direction, except near the midpoint where measurements were taken from above. The impact hammer struck the loop at the same point and in the same direction for every measurement. Using the equilibrium shape and the response associated with the first four frequencies obtained, mode shapes were constructed for each of these frequencies.

4. Results

The cases $\beta = \pi/2, 0$, and $-\pi/2$ will be designated the upright, horizontal, and hanging loop, respectively. Unless otherwise noted, the experimental results will be associated with a strip of cross-sectional dimensions 25.4 mm × 0.508 mm, which corresponds to the reference length a in Eqs. (1) being equal to 0.167 m, and the nondimensional vibration frequency ω being equal to 0.130 times the dimensional frequency. Most of the results will be presented in terms of nondimensional quantities defined in Eqs. (1), in particular length l, frequency ω, and coordinates x and y of the midpoint (where $s = 0.5l$).

Equilibrium results are considered first. Fig. 2 shows the horizontal and vertical components of the midpoint location as a function of length for the horizontal loop. The continuous lines represent the analytical solution and the circles represent the experimental data. The solid line and

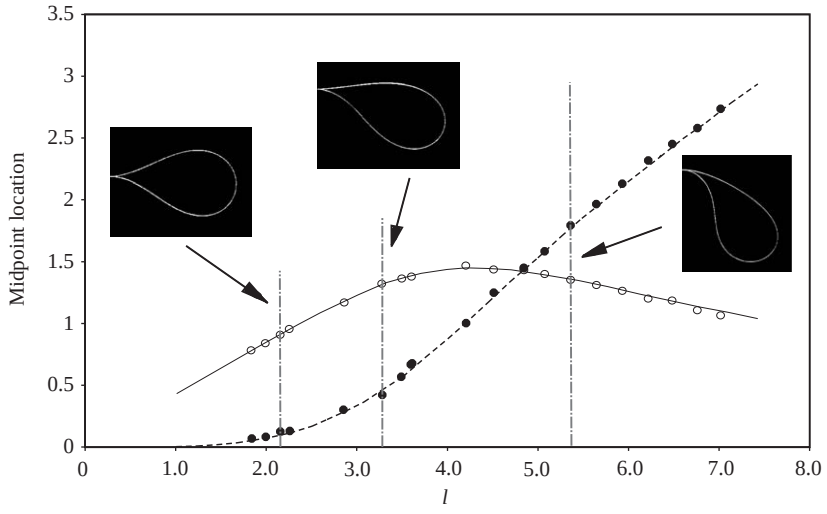

Fig. 2. Midpoint location of horizontal loop (relative to clamped end) as a function of length. Continuous line, horizontal (analytical); dashed line, downward (analytical); •, vertical (experimental); ○, horizontal (experimental).

open circles give the horizontal distance from the clamped end to the midpoint. The dashed line and closed circles denote the downward deflection of the midpoint relative to the height of the clamped end. The downward deflection increases with increasing length, whereas the horizontal distance of the midpoint from the clamped end increases and then decreases. Sample digital images of the experimental equilibrium shapes are shown for $l = 2.15, 3.28$, and 5.36 (denoted by vertical lines).

Equilibrium results for the upright loop are depicted in Fig. 3. The horizontal deflection of the midpoint is plotted as a function of the length of the loop. The critical length is $l = 4.50$ from the analytical solution, and a supercritical pitchfork bifurcation is observed. Also shown in Fig. 3 is a photograph of the loop for $l = 5.29$, when the horizontal midpoint deflection is near its maximum value. The experimental data points are very close to the analytical curve except just beyond this point on the equilibrium path.

Vibration results are presented next. A typical experimental frequency spectrum is depicted in Fig. 4, obtained using the laser vibrometer discussed in the previous section. The upright strip is 0.5096 m long ($l = 3.06$). The results were averaged over four time series. The four lowest dimensional frequencies are distinct at 1.81, 10.73, 20.16, and 30.53 Hz. This procedure was repeated for several thicknesses and a number of lengths. The four lowest measured frequencies are denoted by circles, squares, and triangles in Fig. 5 over a range of nondimensional lengths. Values of the nondimensional frequency ω should not be affected by the thickness of the strip. Continuous curves represent the analytical results. The experimental data points lie very close to the analytical curves.

The mode shapes also were determined for some cases experimentally and analytically. The first four mode shapes for the upright case with $l = 3.48$ and a strip thickness of 0.508 mm are depicted in Fig. 6, along with the equilibrium shape. The corresponding measured dimensional frequencies are 1.3, 8.26, 15.8, and 23.9 Hz. As expected, the second and fourth modes are symmetric with respect to the vertical axis. The theoretical and experimental mode shapes are in close agreement.

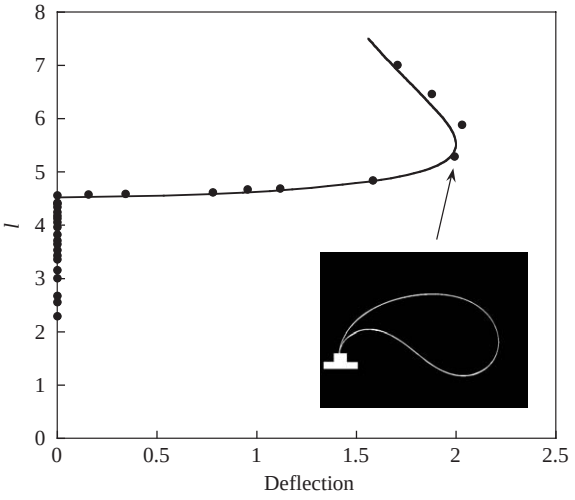

Fig. 3. Horizontal midpoint deflection of upright loop as a function of length. Continuous line, analytical; •, experimental.

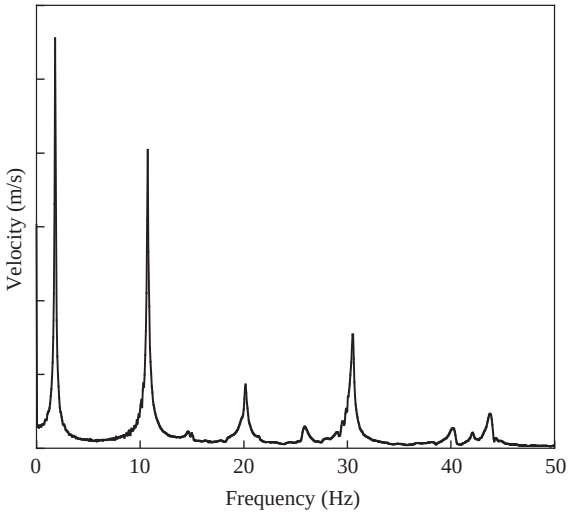

Fig. 4. Typical frequency spectrum for upright loop with $l = 3.06$; main peaks at 1.81, 10.73, 20.16, 30.53 Hz.

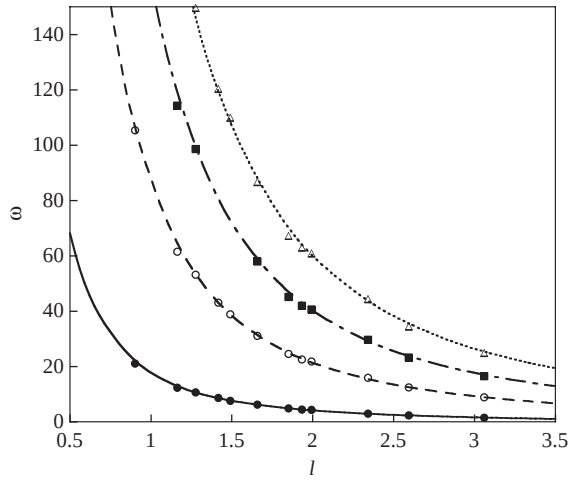

Fig. 5. Lowest four natural frequencies of upright loop as a function of length. Symbols are experimental data points, lines are theory. First mode: • and continuous line; Second mode: ○ and dashed line; Third mode: black squares and dot-dashed line; Fourth mode: △ and dotted line.

Finally, vibrations were studied for loops with different orientations. Results were obtained for angles $\beta = \pi/2$ (upright), $\pi/4$, 0 (horizontal), $-\pi/4$, and $-\pi/2$ (hanging). The lowest (i.e., fundamental) frequency is plotted in Fig. 7 as a function of the nondimensional length, except for the case $\beta = -\pi/4$ since its frequencies are very close to those for $\beta = -\pi/2$. The experimental data points were obtained as the average values from multiple frequency spectra. They lie very close to the analytical results given by the curves.

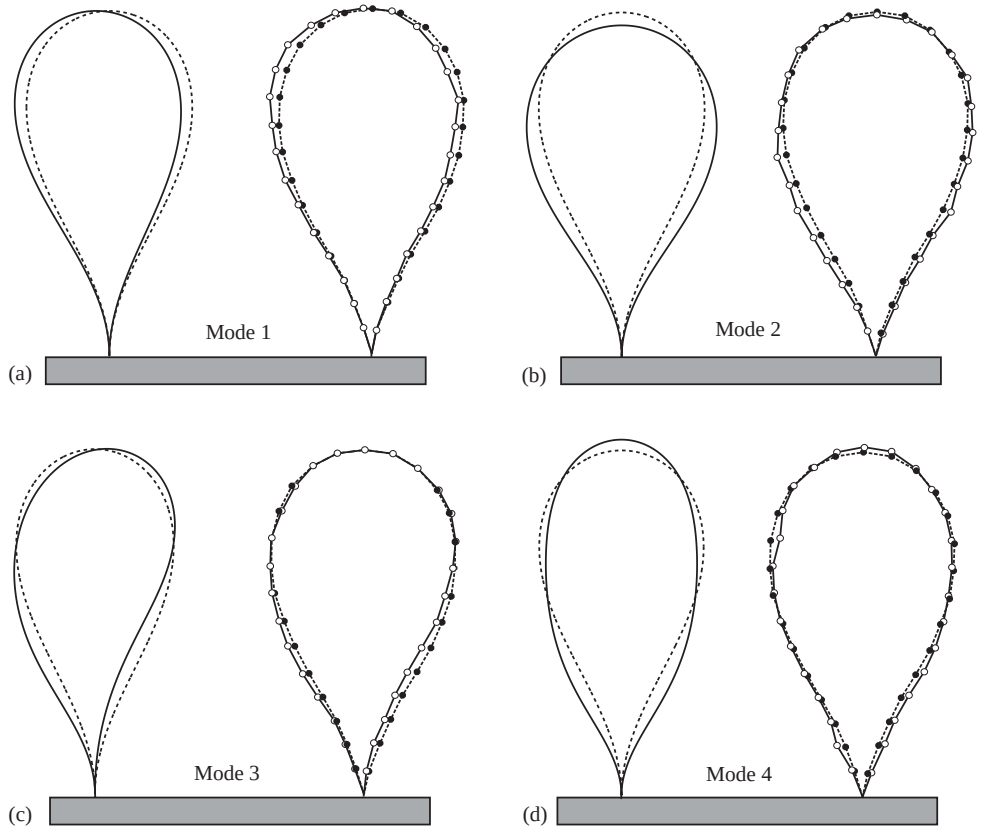

Fig. 6. First four mode shapes for upright loop. (a) Mode 1, (b) mode 2, (c) mode 3, (d) mode 4. Dashed curve, equilibrium (analytical); continuous curve, mode (analytical); •, equilibrium (experimental); ○, mode (experimental).

For the upright loop, as the length of the loop is increased, the fundamental frequency decreases until it is zero at the critical length $l = 4.50$. (Extrapolation of measured fundamental frequencies at smaller lengths to the length at zero frequency could be used to predict the critical length [11].) As the length is increased further and the loop droops (postbuckling deformation), the fundamental frequency increases. For the other orientation angles considered, the fundamental frequency decreases continuously for the range of lengths shown. If angles very close to $\beta = \pi/2$ were considered and l were increased, the corresponding fundamental frequency would decrease until l approached 4.50 and then would increase (similarly to the typical behavior of a slightly imperfect system).

It is noted in Fig. 7 that, for a fixed length of the loop, a reduction in the angle β at the clamped end implies an increase of the fundamental frequency. This is not surprising, since the axial internal force in the loop would tend to become less compressive or more tensile. The differences between the fundamental frequencies for the different orientation angles are small if the length of the loop is either sufficiently small or sufficiently large (i.e., the fundamental frequency becomes almost independent of the orientation).

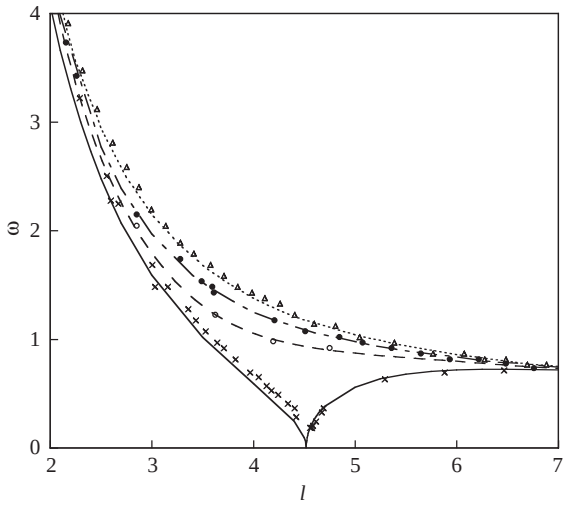

Fig. 7. Fundamental frequency as function of length. Lines are theoretical, symbols are experimental. Continuous and $\times, \beta = \pi/2$; long dashes and $\circ, \beta = \pi/4$; dot-dashed and $\bullet, \beta = 0$; dotted and $\triangle, \beta = -\pi/2$.

5. Concluding remarks

A pinched loop was considered, with various orientations of its clamped end. Equilibrium shapes and small in-plane vibrations about those shapes were examined analytically and experimentally. In the analysis, the weight of the loop was included, but damping was neglected. The loop was treated as an elastica and solutions were obtained with a shooting method. In the experiments, polycarbonate strips were used. The orientation was fixed and the length of the loop was increased.

The behavior depends on the orientation and length of the loop. Buckling is only possible for the upright loop: in-plane buckling occurs at a critical length, and the loop droops smoothly to one side as the length is increased further. If the loop hangs vertically downward, the equilibrium configuration remains symmetric and an increase of length causes the shape to become slightly thinner and longer. For any other orientation, the droop increases as the length is increased.

The first vibration mode corresponds to a rocking about the equilibrium configuration, essentially pivoting about the clamped end. For the upright loop and the hanging loop, if the modes are numbered according to the order of the frequencies, the even-numbered modes are symmetric about the vertical axis.

The correlation between the analytical and experimental results was very good, both for equilibrium shapes and the first four vibration frequencies and modes. In a related problem, an upright half-loop was considered in Ref. [12], with the clamped ends oriented vertically and separated by a fixed distance. The cross section was circular, rather than the thin cross section of the strip considered above. As the length of the half-loop was increased, out-of-plane buckling occurred at a critical length. The buckling was smooth (supercritical bifurcation) if the material was linearly elastic, but if the material had a sufficient amount of softening, the half-loop suddenly

jumped from a planar shape to a severely drooped out-of-plane configuration when the critical length was reached (subcritical bifurcation).

Acknowledgements

This research was supported by the US National Science Foundation under Grant no. CMS-0301084.

References

[1] R.H. Plaut, N.L. Williams, D.A. Dillard, Elastic analysis of the loop tack test for pressure sensitive adhesives, *Journal of Adhesion* 76 (2001) 37–53.
[2] Y. Woo, R.H. Plaut, D.A. Dillard, S.L. Coulthard, Experiments and inelastic analysis of the loop tack test for pressure-sensitive adhesives, *Journal of Adhesion* 80 (2004) 203–221.
[3] J.E. Flaherty, J.B. Keller, Contact problems involving a buckled elastica, *SIAM Journal on Applied Mathematics* 24 (1973) 215–225.
[4] R.H. Plaut, R.P. Taylor, D.A. Dillard, Postbuckling and vibration of a flexible strip clamped at its ends to a hinged substrate, *International Journal of Solids and Structures* 41 (2004) 859–870.
[5] G. Domokos, W.B. Fraser, I. Szeberényi, Symmetry-breaking bifurcations of the uplifted elastic strip, *Physica D* 185 (2003) 67–77.
[6] R.H. Plaut, S. Suherman, D.A. Dillard, B.E. Williams, L.T. Watson, Deflections and buckling of a bent elastica in contact with a flat surface, *International Journal of Solids and Structures* 36 (1999) 1209–1229.
[7] N.C. Perkins, Planar vibration of an elastica arch: theory and experiment, *Journal of Vibration and Acoustics* 112 (1990) 374–379.
[8] T.B. Bahder, *Mathematica for Scientists and Engineers*, Addison-Wesley, Reading, MA, 1995.
[9] S. Wolfram, *The Mathematica Book*, third ed., Cambridge University Press, Cambridge, UK, 1996.
[10] C.-Y. Wang, Folding of elastica—similarity solutions, *Journal of Applied Mechanics* 48 (1981) 199–200.
[11] R.H. Plaut, L.N. Virgin, Use of frequency data to predict buckling, *Journal of Engineering Mechanics* 116 (1990) 2330–2335.
[12] R.H. Plaut, L.N. Virgin, Three-dimensional postbuckling and vibration of vertical half-loop under self-weight, *International Journal of Solids and Structures* 41 (2004) 4975–4988.